electronics

MDPI

Article

Reliability Evaluation of LED Lamp Beads Considering Multi-Stage Wiener Degradation Process Under Generalized Coupled Accelerated Stress

Yinglong Dong [1], Zhen Zhou [1,*], He Dai [2] and Kaixin Liu [3]

[1] School of Measurement and Communication, Harbin University of Science and Technology, Harbin 150080, China; 1810600001@stu.hrbust.edu.cn
[2] School of Automation, Harbin University of Science and Technology, Harbin 150080, China; 2220510118@stu.hrbust.edu.cn
[3] Institute of Performance and Test Technology, General Machine Tool Research Institute, Beijing 101318, China; liukaixin2@gt.cn
* Correspondence: zhzh49@126.com

Abstract: LED lamp beads (hereinafter referred to as LEDs) are complex electronic components, and their degradation process shows multi-stage characteristics. Ignoring the effects of multi-stage degradation and stress coupling will lead to a higher theoretical lifespan. In this paper, a Wiener process model based on generalized coupling is proposed for the staged degradation of LEDs. This paper first conducts accelerated degradation tests on LEDs under different temperature, humidity, and current stress combinations to obtain three index parameters of LEDs. Light output performance (LOP) is selected as the degradation characteristic quantity, and the Shapiro–Wilk test is used to determine whether the parameters conform to the normal distribution. Then, the unknown parameters of the multi-stage Wiener process are estimated and a generalized coupling model is established using the unknown parameters and accelerated degradation test data. Finally, the LED life under standard stress is extrapolated based on the multiple stress acceleration factors. The analysis of LED reliability experimental data shows that the proposed method can realize reliability assessment and has higher lifetime prediction accuracy compared with the multi-stage model without considering stress coupling.

Keywords: LED; multi-stress coupling; Wiener process; reliability; acceleration factor

Citation: Dong, Y.; Zhou, Z.; Dai, H.; Liu, K. Reliability Evaluation of LED Lamp Beads Considering Multi-Stage Wiener Degradation Process Under Generalized Coupled Accelerated Stress. *Electronics* **2024**, *13*, 4724. https://doi.org/10.3390/electronics13234724

Academic Editor: Francesco Giuseppe Della Corte

Received: 22 October 2024
Revised: 18 November 2024
Accepted: 26 November 2024
Published: 29 November 2024

1. Introduction

As key components of electronic equipment such as communication, sensing, and optoelectronic coupling, LEDs' reliability evaluation and life assessment are of great importance for enhancing the performance and health monitoring of electronic equipment. High reliability has become a prominent feature of the current service life in the field of LED engineering. While it is becoming more and more difficult for LED products to fail, this factor is also accompanied by an increase in the difficulty of obtaining exact life data. Therefore, performance degradation analysis provides a feasible way for product life prediction and reliability assessment. The performance degradation analysis method not only removes the drawbacks of over reliance on life data but also deeply mines the reliability information hidden in the degradation quantity. Therefore, it is very important to apply a suitable model to match the performance degradation trajectory of LEDs. Common modeling methods can be mainly divided into three categories: physical model, deep learning model, and degradation quantity distribution model. The physical model requires a specific analysis of the internal operating mechanism and external use conditions of the equipment. The evaluation accuracy is high, but the universality of the model is poor, and it is difficult to cover the specific conditions in other fields [1,2]. Deep learning

models are highly inclusive and adaptable, making them well-suited for situations where the degradation process lacks regular patterns. However, when the amount of data is insufficient, they are more likely to overfit, mainly because they perform poorly on unseen data [3]. The modeling method based on degradation quantity avoids the specific analysis of the internal structure and mechanism of the test product and therefore has strong adaptability. Research on the distribution of performance degradation quantity mainly focuses on three directions: random variable method, graph analysis method, and random process method. The random variable method and graph analysis method must assume that the degradation path is certain, and can only be suitable for products with obvious degradation characteristics and simple failure mechanisms. However, the most serious problem is that we ignore the differences in the degradation of the same products under the same conditions. The stochastic process method of degradation is a statistical method grounded in stochastic process theory to describe and model the degradation behavior of products or systems. It predicts the life and failure time of the system by considering degradation as a random variable that evolves. This method is particularly suitable for predicting the life of products that cannot be directly observed through a single stress test, especially under complex and multi-factor degradation mechanisms [4].

At present, many scientists have studied the degradation of LEDs. Mehr found that the stress conditions used are an important factor in the life of LED lamp beads, especially temperature and humidity, but did not take into account the degradation stage and stress coupling of LED chips [5]. Fu-Kwun studied the accelerated degradation test of LED light strips under temperature and current stress but did not consider the coupling effect and degradation stage of LED temperature and current, resulting in an overestimation of their life [6]. Miao studied the life prediction of ultraviolet LEDs under working conditions. Since only temperature was considered as a degradation factor, the maximum error between the estimated life and the actual life at 8000 h was 16%, and the accelerated degradation process of ultraviolet LEDs in the middle was not considered [7]. In research on UV LEDs, Liang used the dual stress of temperature and current for degradation testing but did not test the changes in the failure mechanism of LEDs caused by the step up in temperature and current. The article also did not consider the impact of the temperature–current coupling effect on the life of the UV LEDs after adding the two stresses at the same time [8]. Wang found that LOP degraded into two stages in the stress test of some luminous products, but did not take into account the mutual influence between different stresses [9]. LED testing needs to consider the true correlation between stresses. Failure to consider stress coupling will lead to large deviations in reliability.

The Wiener process model has fewer parameters and higher prediction accuracy, so it is widely used in the degradation modeling of various equipment and materials [10,11]. To solve the heterogeneity in the samples, Si added the standard Brownian motion to the Wiener process, it has good universality, but its applicability to degradation under multi-stress coupling and multi-stage degradation is poor [12]. Li used the Wiener process to predict the life of the main insulation material of the motor but did not consider the degradation stage trend and other stress couplings under temperature stress, which is not suitable for actual application scenarios [13]. To deal with the above-mentioned problems, a reliability evaluation method of the multi-stage Wiener degradation process under generalized coupled accelerated stress is proposed. Based on the analysis of the LED degradation mechanism, LEDs are subjected to accelerated degradation tests under five different constant temperature humidity current stresses. LOP is selected as the degradation characteristic of LEDs. An LED degradation model based on a three-stage Wiener process was established, and the unknown parameters of the model were determined by the maximum likelihood estimation method. According to the parameter estimation of the Wiener process and the accelerated degradation test data, a generalized coupling model based on the Arrhenius model was constructed, and the prediction of LED light output power (LOP) degradation at room temperature was realized through multi-stress acceleration factors. The rest of this article is as follows. The accelerated degradation

test of this study is shown in Section 2. The detailed method of this study is in Section 3. The reliability evaluation and discussion of LEDs are in Section 4. Section 5 summarizes this study.

2. Materials and Methods

2.1. Selection of Accelerated Stress

At high temperatures, the electron mobility of semiconductor materials will degrade, resulting in lower LED luminous efficiency. The mechanical properties of the packaging material will degrade, and microcracks or peeling may occur at the interface between the semiconductor chips, leading to failure. The phosphor, encapsulation resin, and other materials inside the LED will decompose or deteriorate at high temperatures, resulting in reduced luminous efficiency, color drift, and other problems. High humidity will lead to LED packaging material absorbing moisture, causing the internal circuit to become damp, and increasing leakage current. Silicone or epoxy resin may undergo xanthation after absorbing moisture, affecting optical performance and reducing luminous flux output [5]. In long-term high humidity environments, the luminous efficiency of phosphor will decrease, resulting in changes in brightness and color temperature. When LEDs operate at a high current, the luminous efficiency usually decreases, which is called an efficiency droop. A high current will cause the LED to generate a large amount of heat, causing local overheating of the chip. The resulting thermal stress will cause microcracks and physical damage to the chip [14]. Therefore, this paper selected temperature, humidity, and current as accelerated degradation stresses.

2.2. Accelerated Degradation Test Design

The specifications of the LED selected in this article are shown in Table 1. The rated voltage of this LED was 3.3 V, the current was 10 mA, the operating temperature range was −25–60 °C, and the humidity was 40–75%. The manufacturer gave the LED a life of about 20,000 h at 25 °C, 40% humidity, and 10 mA current, which was the standard for this article.

Table 1. Specifications of the LED.

Item	Value
Burden: voltage circuit	3.3 V
Burden: current circuit	10 mA (100 mA)
Temperature	−20–65 °C
Humidity	40–75%

Following TM-28-14 [15], we conducted a single stress 85 °C test for 6000 h. Since the LED life under single temperature stress may be about 12,000 h, the test time at too low a temperature was too long, which increased the experimental time cost. According to the literature [16], five different stress combinations of degradation tests were selected, as shown in Table 2. Under actual working conditions, the chip P-type electrode and P-finger burned, and the N-finger burned abnormally. The failure mechanism of the LED selected under the five stresses was consistent with the failure mechanism of the LED in reality. However, whether it is possible to increase the stress level and reduce the time loss while keeping the failure mechanism unchanged is also a future research direction.

Table 2. Test conditions.

No.	Temperature (°C)	Humidity (%)	Current (mA)
S1	85	45	20
S2	85	85	20
S3	85	85	220
S4	95	45	525
S5	150	45	300

Three different temperature gradients were selected, mainly because the combination of high temperature and high current cannot change the failure mechanism of LEDs. Humidity has two gradients: normal humidity and high humidity. The four current gradients are better for reflecting the coupling effect with other stresses. Considering that if one LED fails during the test, according to the confidence level of 0.8 and the sample confidence of 95%, the number of samples n for the five groups of tests S1–S5 should be greater than or equal to 59 [17]. Since the test PCB board was a group of 10 LEDs, that is, each group of S1–S5 used 60 LEDs for testing, a total of 300 LEDs from the same manufacturer and the same batch were tested.

2.3. Accelerated Degradation Test

According to the TM-28-14 standards, three types of data—light output performance, forward voltage, and cut-in voltage—were measured after each test cycle.

Light output performance (LOP) is an important indicator for evaluating the light output characteristics of LEDs or other light sources. When the LOP of an LED drops to 70% of the initial value under certain conditions, the LED is considered to have failed. The usage time under this condition is the LED life, marked as L70. To maintain the consistency of the tested LEDs, the ones with similar initial brightness are selected as a group. BE (basic error) is the deviation between the measured LOP of the LED and its initial LOP, defined as the following Equation (1). In this paper, LEDs were declared failed when LOP BE was 0.695.

$$BE = \frac{LOP_{test} - LOP_{\text{int}}}{LOP_{\text{int}}} \quad (1)$$

The forward voltage (V_F) of an LED can change over time, especially during the aging process. As time goes by, the internal structure of the LED may change, causing the forward voltage to increase or decrease. Monitoring this value can help predict the life of the LED.

The cut-in voltage (V_{Fin}) generally refers to the voltage value under a small current (close to the turn-on voltage), that is, the test current is 1 uA, at which no thermal effect occurs. It mainly reflects the consistency ability of the LED chip, the defect status of the epitaxial (PN junction part), etc. That is, under the 1 uA test condition, the larger the value, the better. Taking the LED chip in this paper as an example, when it was less than 2 V, it could be considered that the LEDs had failed.

Before starting the experiment, due to the differences in LEDs, it was necessary to first obtain each LED's initial light output power (LOP) value. Figure 1 below shows a complete test cycle.

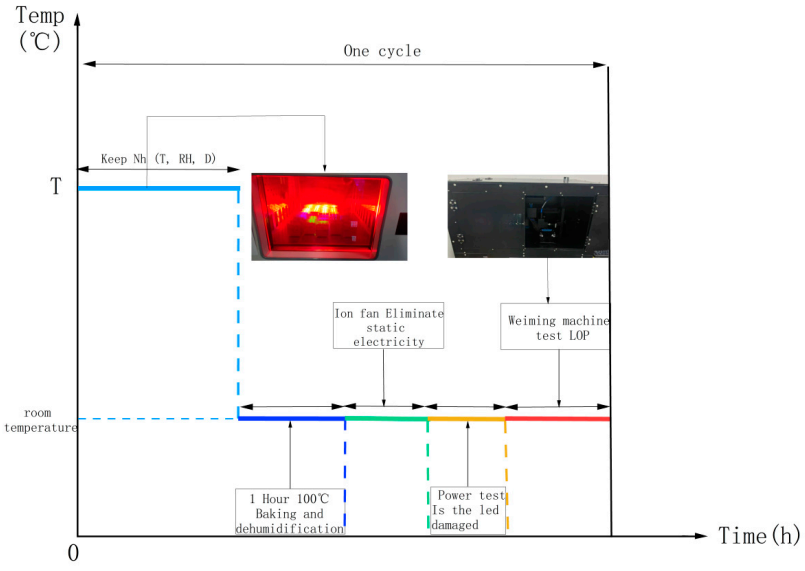

Figure 1. Overview of a testing cycle.

1. The LEDs were put into the Nissoku programmable constant temperature and humidity tester, and degradation tests were performed on 6 groups of PCB boards (10 LEDs per group) according to certain conditions according to the degradation data collection time under each stress shown in Table 3.

Table 3. Degeneration data acquisition time under different stresses.

Test Stress Level	Time of Data Measurement/h
S1 (85 °C 45%RH 20 mA)	0, 24, 72, 119, 168, 313, 532, 699, 867, 1033, 2091, 3105, 4416, 5420, 6427, 6523, 6619, 6751, 6811, 6907, 7003, 7195, 7387
S2 (85 °C 85%RH 20 mA)	0, 24, 72, 119, 168, 313, 532, 699, 867, 1033, 1149, 1319, 1487, 1846, 2091, 2895, 3105, 4416, 5420, 6427, 7387, 7430
S3 (85 °C 85%RH 220 mA)	0, 24, 72, 119, 168, 313, 532, 699, 867, 1033, 1149, 1319, 1487, 1750, 1846, 2091, 2283, 2475, 2895, 3105
S4 (95 °C 45%RH 525 mA)	0, 24, 72, 120, 168, 216, 264, 312, 360, 408, 456, 504, 552, 600, 648, 696, 744, 792, 840, 888, 936, 984, 1032, 1080
S5 (150 °C 45%RH 300 mA)	0, 24, 72, 120, 168, 216, 264, 312, 360, 408, 456, 504, 552, 600, 648, 696, 744, 792, 840, 888, 936, 984

2. In order to prevent condensation between the damp PCB and the air, which may cause unexpected failures of the LEDs, the PCB needed to be baked for 1 h for dehumidification when performing S2 and S3 of the high humidity test.

3. Ion fans were used to neutralize static electricity on the PCB, as static discharge may cause LEDs to break down.

4. In many cases, even though there is no physical damage or burn marks on the LEDs, the LEDs fail due to limitations in the formation of crystal defects in the chip epitaxial layer structure [18]. In this case, a multimeter was needed to test whether the LEDs were damaged.

5. The six PCB boards were placed into the Weimin tester to test the light output performance, forward voltage, and cut-in voltage of the LEDs.

2.4. Data from an Accelerated Degradation Test

Since the degradation of a single case is random, 60 LED samples were used under each stress. Each test cycle of S1–S5 needed to measure the three indicators of LEDs: V_F, V_{Fin}, and LOP BE. The horizontal axis in Figure 2a–e is time. It should be noted that the time shows the measurement time in Table 3. The time axis in Figure 2f is the normal time axis. The *y*-axis of Figure 2a,b is VF, the *y*-axis of Figure 2c,d is V_{Fin}, and the *y*-axis of Figure 2e,f is LOP BE. Figure 2a shows the VF degradation of LEDs under S1 stress, where S11 represents the first test LED under S1 stress, and avr represents the average VF value of the 9 LEDs in this group. Figure 2b shows the VF degradation of 9 LEDs under S3 stress, and avr represents the average VF value of the 9 LEDs in this group. Figure 2c shows the V_{Fin} degradation of 9 LEDs under S2 stress, and avr represents the average VF value of the 9 LEDs in this group. Figure 2d shows the V_{Fin} degradation of 9 LEDs under S4 stress, and avr represents the average V_{Fin} value of the 9 LEDs in this group. Figure 2e shows the LOP BE degradation of 9 LEDs under S5 stress, and avr represents the average LOP BE value of the 9 LEDs in this group. Figure 2f shows the average LOP BE degradation of 60 LEDs in each group under S1–S5 stress.

As depicted in Figure 2a, under the S1 stress condition, the V_F of LEDs varied from 3.303 V to 3.399 V, and S14 stopped at 6523 h because S14 was in a failed state at that moment. The last acquisition time of S11-S19 was the failure life of the LED. As shown in Figure 2b, S31, S32, and S39 had voltage mutations at 1033 h, 1149 h, and 3105 h, respectively. In the following tests of 1149 h, 1319 h, and 3297 h, V_F = 19.999 V, that is, the LEDs were burned out, and LOP BE was −1. As can be seen from Figure 2a,b, the degradation of V_F in LEDs was not obvious, and it was not suitable as a degradation of LEDs. However,

it is a good research direction to find out the accidental failure of LEDs in advance by measuring V_F; however, the measurement time interval and the sporadic occurrence may be issues to be considered. Figure 2c shows the change of V_{Fin} over time under S2 stress. S21 and S25 experienced sudden changes at 1149 h and 2091 h, and the LED was directly short-circuited, resulting in a measured voltage of 19.999 V. S29 experienced a sudden change in V_{Fin} at 7387 h and a short circuit occurred at 7430 h. Figure 2d shows that S41 experienced a sudden change in V_{Fin} at 552 h, S42 and S43 at 696 h, and S49 experienced an LED short-circuit at 1080 h, resulting in a V_{Fin} of 19.999 V. It should be noted that only S29 experienced a sudden change in V_{Fin} before the occasional failure, but it may also be that the change was not collected due to different measurement times. From Figure 2c,d, it is evident that V_{Fin} was not degraded.

LOP BE is a degradation characteristic quantity of LEDs, which has a clear trend of LED degradation and is strongly correlated with stress levels. Figure 2f shows the average LOP BE variation trend of S1–S5 under different temperatures, humidity, and current stresses. The figure shows that the difference in life grew as the stress level increased, among which temperature stress was the most obvious. In Figure 2f, we can see that, under S1–S3 stress, LEDs' LOP BE had obvious stage changes. Although the degradation stage under S4 and S5 high stress was not very obvious, it can also be seen that LED degradation was staged. Under S1–S3 stress, LED degradation was slow in stage 1, accelerated in stage 2, and slow in stage 3. The early degradation under S4 and S5 stress was relatively short. To better understand the degradation mode of LEDs' LOP BE, Figure 3a–e show 300 sample LEDs under S1–S5 stress/three-stage LOP BE.

In Figure 3a–e above, the degradation of LEDs under S1–S5 stress is shown. The horizontal axis is the degradation time, the vertical axis is the number of samples, the *z*-axis is the LOP BE degradation, and the 20th sample on the vertical axis is the average degradation of all 60 samples. In the LED LOP BE degradation, we found that the LED degradation had three stages. To better show the stage changes, the internationally common warning colors of blue, yellow, and red were used to represent the initial degradation, accelerated degradation, and late degradation. The specific inflection point position is introduced in 3.3 of this paper. Notably, under S1 stress, we observed that the change in LOP for the first 2091 h of the LEDs was positive. Under S2 stress, the LOP BE change of LEDs in the first 1033 h was positive, and the brightness exceeded the initial value. During the 24 h to 72 h of S5 stress and the 120 h to 168 h of S4 stress, the rate of change in LOP BE also rose, but the LOP BE was not positive. The reason is that the newly produced LEDs may not have fully stabilized internal materials in the initial working stage. When the LED was activated, the electrons and holes inside may have rearranged, causing the light output to gradually increase until it reached a stable state. Under S5 stress, there was also an initial two-level differentiation. At 0–24 h, the LOP BE range was -0.0038 to -0.0864. There was a group of 10 samples with a specific range of -0.0038 to -0.0096, and the remaining 50 samples had a range of -0.0597 to -0.094. This is also reflected in Figure 2e. However, it returned to normal values during the 24–72 h test. The specific reason is not yet known. It may be that the problems in the test process of this group of experiments caused the abnormal situation of this group of data. This paper temporarily calculates the correct data according to the values of this group.

To better understand the degradation of LOP BE of LEDs under various stresses, we plotted the following Figure 4.

In Figure 4, the horizontal axis is the degradation time, the vertical axis is the five stresses S1–S5, and the *z*-axis is the degradation amount. The large figure shows the average degradation curves of the five stresses S1–S5 LOP BE, where the blue solid points are the change points in three different stages, connected by black dotted lines. Since the degradation time of S4 and S5 was relatively short, it is difficult to see the position of the change points in the 3D graph, so the average degradation curves of S4 and S5 are drawn in the upper left corner of Figure 4, and the blue solid points are marked as change points.

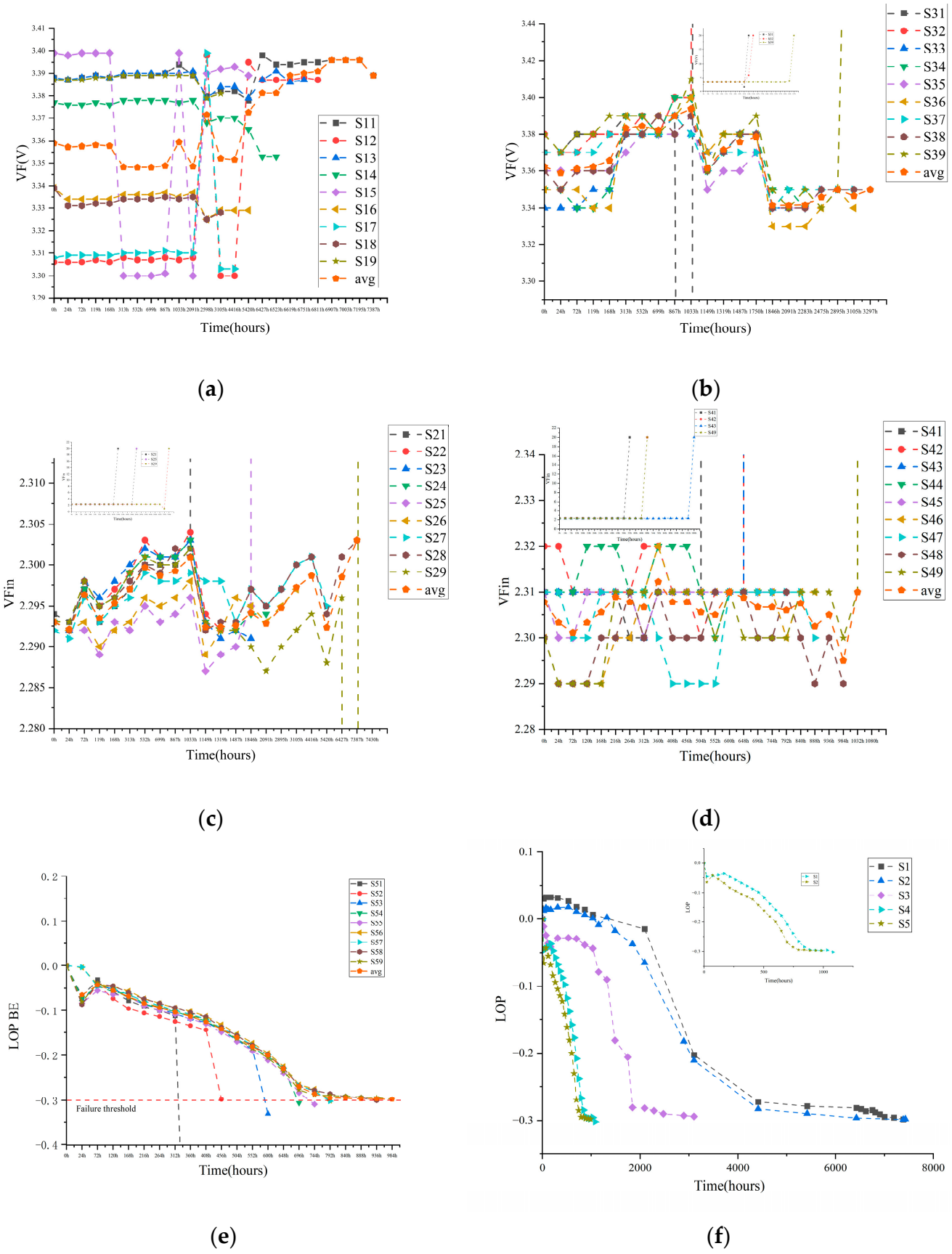

Figure 2. (**a**,**b**) are the degradation trends of LEDs' V_F, (**c**,**d**) are the degradation trends of LEDs' V_{Fin}, (**e**,**f**) is the degradation trend of LEDs' LOP BE.

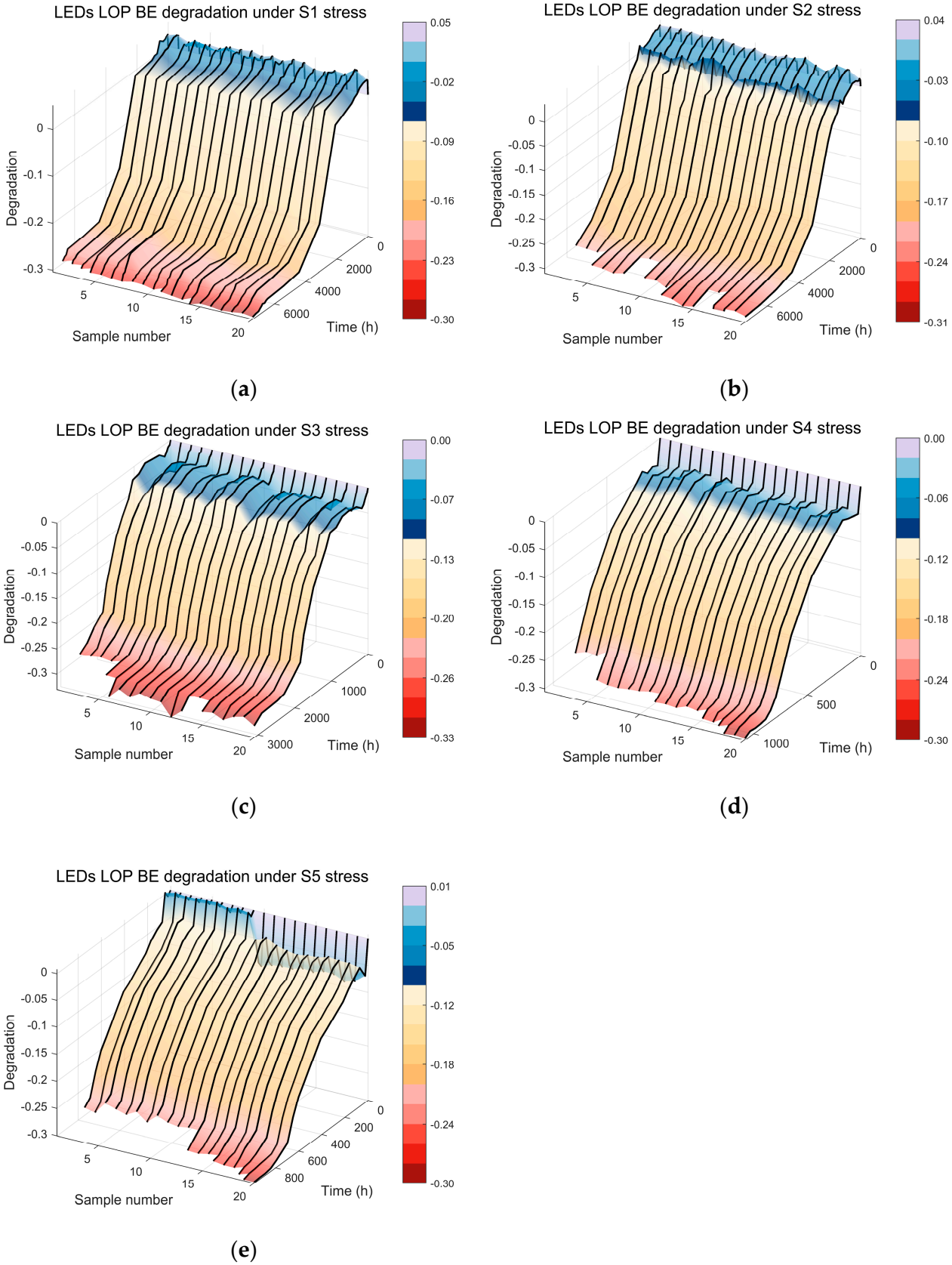

Figure 3. Three hundred sample LEDs under S1-S5 stress/three-stage LOP BE. Among them, (**a**) is the LOP degradation diagram under S1 stress, (**b**–**e**) are the LOP degradation diagrams under S2–S5 stresses respectively.

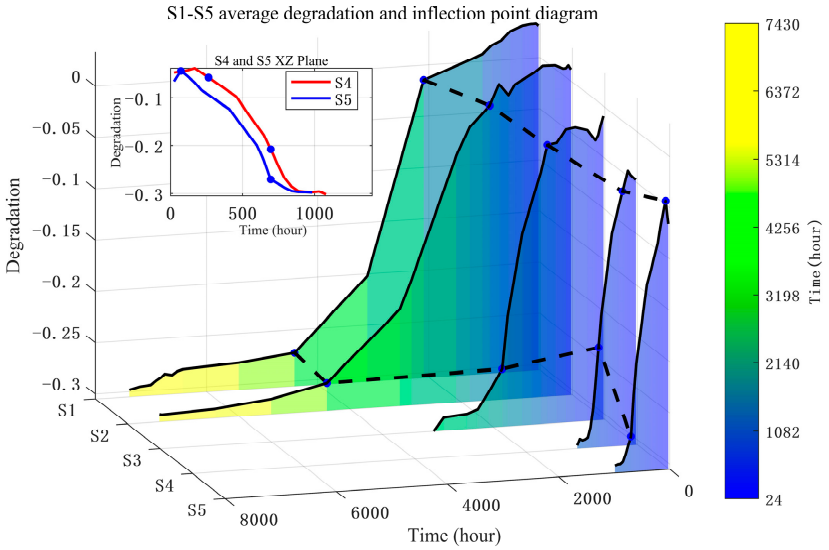

Figure 4. Connection lines of LOP BE of three-stage samples under S1–S5 stress and their corresponding stage change points.

3. LED LOP BE Degradation Modeling

3.1. Degradation Model Selection

Since the degradation of LEDs' LOP BE is caused by the accumulation of a large number of tiny losses, it can be considered to be modeled using a univariate Wiener process [18]. The internal structure of the LED is corroded by thermal, electrical, and moisture stresses over a long span, and the reduction in life expectancy is due to the accumulation of a large number of tiny losses, which also conforms to the characteristics of the Wiener process. The Brownian motion in the Wiener process can incorporate the randomness and contingency of the LED operation process into the model. Therefore, the article selects a model grounded in the Wiener process that can reflect cumulative and random degradation as the degradation model of LEDs. The degradation model selects a univariate Wiener process, and the feature quantity X(t) must satisfy the following three assumptions:

1. The increment between any period $[t, t+\Delta t]$ follows a normal distribution, that is, $X(t+\Delta t) - X(t) \sim N(\mu\Delta t, \sigma^2\Delta t)$.
2. In any two non-intersecting periods during the degradation process, $[t_1, t_2]$ and $[t_3, t_4]$, that is, $t_1 < t_2 \leq t_3 < t_4$, increments $X(t_2) - X(t_1)$ and $X(t_4) - X(t_3)$ are mutually independent.
3. $P(X(0) = 0) = 1$. This means that the univariate Wiener process is determined from its value at time t = 0 to be 0, which is an initial condition.

If the degradation process that we consider has random factors, then the univariate linear Wiener process model with drift is as follows in Equation (2):

$$X(t) = X(0) + \theta t + \sigma W(t) \tag{2}$$

where t is the degradation time, $X(0)$ is the initial degradation amount, θ is the drift parameter, which refers to the average rate of change of the degradation characteristic. σ is the diffusion parameter, which represents the randomness of the change and reflects the influence of random factors such as measurement error and noise on the degradation during degradation. $W(t)$ is the standard Wiener process. $X(t)$ represents the total accumulated degradation of the LED's LOP at the moment t.

In this paper, LED LOP BE was selected as the degradation characteristic quantity, and LOP BE needed to be tested for normality before degradation modeling.

3.2. Multi-Stage Degradation Modeling Based on the Wiener Process

For LEDs, the degradation process of their entire life cycle presents multi-stage characteristics. In other words, the degradation rate of LEDs' performance indicators will change significantly in the early, middle, and late stages of degradation. Using a single Wiener process cannot accurately express its degradation performance. Therefore, this paper proposes a multi-stage degradation process model based on the Wiener process. The LED degradation process needs to meet the following assumptions:

1. When the LED's LOP BE $X(t)$ reaches the failure threshold D = 0.695 for the first time, the equipment is considered to have failed.

The reliability function $R(t)$ of the system is the likelihood that the system remains operational up until time t. This probability can be expressed as the following Equation (3):

$$R(t) = P(X(t) < D) \tag{3}$$

To the probability of $R(t)$, it needs to consider the degradation process within each stage and across stages separately.

2. The degradation process of the device conforms to the multi-stage degradation form. Assume that the device goes through k stages, and each stage has different drift and diffusion parameters. The specific model can be expressed as following Equation (4):

$$\begin{cases} X(0) + \theta_1 t + \sigma_1 W(t), & 0 \le t < \tau_1 \\ X(\tau_1) + \theta_2 (t - \tau_1) + \sigma_2 (W(t) - W(\tau_1)), & \tau_1 \le t < \tau_2 \\ \vdots & \vdots \\ X(\tau_{k-1}) + \theta_k (t - \sigma_{k-1}) + \sigma_k (W(t) - W(\tau_{k-1})) & \tau_{k-1} \le t \end{cases} \tag{4}$$

The time point when the stage i ends is time τ_i.

According to the above Equation (4), the three-stage Wiener process model is as follows:

Stage 1: $(0 \le \mathrm{t} < \tau_1)$

In the first stage, the degradation process just follows a simple Wiener process as described by the following Equation (5):

$$X_1(t) = X(0) + \theta_1 t + \sigma_1 W(t) \tag{5}$$

At this time, the probability density function $f_{X_1}(x, t)$ of the process is the probability density function of the standard Wiener process as follows in Equation (6):

$$f_{X_1}(x, t) = \frac{1}{\sqrt{2\pi\sigma_1^2 t}} \exp\left(-\frac{(x - X(0) - \theta_1 t)^2}{2\sigma_1^2 t} \right) \tag{6}$$

The reliability function of LED in stage 1 is as follows Equation (7):

$$R_1(t) = P(X(t) < D) = P\left(\frac{X(0) + \theta_1 t - D}{\sigma_1 \sqrt{t}} < \frac{W(t)}{\sqrt{t}} \right) = \Phi\left(\frac{D - X(0) - \theta_1 t}{\sigma_1 \sqrt{t}} \right) \tag{7}$$

where $\Phi(\cdot)$ is the standard normal distribution function.

Stage 2: $(\tau_1 \le t < \tau_2)$

The degradation of LED LOP in stage 1 will affect the degradation in stage 2. The expression of stage 2 is as follows in Equation (8):

$$X_2(t) = X(\tau_1) + \theta_2 (t - \tau_1) + \sigma_2 (W(t) - W(\tau_1)) \tag{8}$$

Since $X(\tau_1)$ is a random variable, the probability density function in stage 2 needs to be expressed by conditional density. Assuming that we already know $X(\tau_1) = x_1$, the conditional probability density function of $X_2(t)$ is as follows in Equation (9):

$$f_{X_2|X(\tau_1)=x_1}(x,t) = \frac{1}{\sqrt{2\pi\sigma_2^2(t-\tau_1)}} \exp\left(-\frac{(x-x_1-\theta_2(t-\tau_1))^2}{2\sigma_2^2(t-\tau_1)}\right) \tag{9}$$

The reliability function of LED in stage 2 is as follows in Equation (10):

$$R_2(t) = \Phi\left(\frac{D - X(\tau_1) - \theta_2(t-\tau_1)}{\sigma_2\sqrt{t-\tau_1}}\right) \tag{10}$$

where $X(\tau_1) = x_1$ is the solution obtained by combining the results of the first stage.

Stage 3: $(\tau_2 \leq t)$

In stage 3, the degradation process continues to be affected by the first two stages, as expressed in Equation (11):

$$X_3(t) = X(\tau_2) + \theta_3(t-\tau_2) + \sigma_3(W(t) - W(\tau_2)) \tag{11}$$

Similarly, when $X(\tau_2) = x_2$ is given, the conditional probability density function of $X_3(t)$ is as follows in Equation (12):

$$f_{X_3|X(\tau_2)=x_2}(x,t) = \frac{1}{\sqrt{2\pi\sigma_3^2(t-\tau_2)}} \exp\left(-\frac{(x-x_2-\theta_3(t-\tau_2))^2}{2\sigma_3^2(t-\tau_2)}\right) \tag{12}$$

The reliability function of the system at this stage 3 is as follows in Equation (13):

$$R_3(t) = \Phi\left(\frac{D - X(\tau_2) - \theta_3(t-\tau_2)}{\sigma_3\sqrt{t-\tau_2}}\right) \tag{13}$$

Similarly, since $X(\tau_2)$ is the cumulative result of the first two stages, we need to consider the entire process comprehensively.

3.3. Change Point Detection

The process of judging whether a model has a change point is the process of selecting a model. SIC (Schwarz information criterion) change point detection is a statistical method used in time series analysis to identify structural change points in a sequence. The principle is that the entropy of its sample is greater than the entropy of the sample without a change point, which is defined as the following Equation (14):

$$\mathrm{SIC} = -2\ln(L) + k\ln(n) \tag{14}$$

where L is the maximum likelihood function of the model, k is the quantity of parameters in the model, including the location of the change point. n is the number of samples. According to the SIC principle, to identify the point of change, the following assumptions are made in this paper:

Null assumption H_0: the parameter values are equal, that is, there is no change point in the model. Alternative assumption H_1: there is a change point τ; before τ it degenerates to $X_1\left(t;\mu_1,\sigma_1^2\right)$, after τ it degenerates to $X_2\left(t;\mu_2,\sigma_2^2\right)$. Then, according to the above Equation (14), $\mathrm{SIC}(n)$ under the original assumption H_0 is the following Equation (15):

$$\mathrm{SIC}(n) = n\ln 2\pi + n\ln\sum_1^n(\Delta x_i - \Delta\overline{x})^2 + n + (2-n)\ln n \tag{15}$$

where $\Delta\overline{x} = \frac{1}{n}\sum_{1}^{n}\Delta x_i$.

SIC(k) under the alternative assumption H_1 is as follows Equation (16):

$$\mathrm{SIC}(k) = n\ln 2\pi + k\ln\frac{1}{k}\sum_{1}^{n}(\Delta x_i - \Delta\overline{x}_1)^2 + 4\ln n + (n-k)\ln\frac{1}{n}\sum_{k+1}^{n}(\Delta x_i - \Delta\overline{x}_2)^2 - n \quad (16)$$

where $\Delta\overline{x}_1 = \frac{1}{k}\sum_{1}^{k}\Delta x_i$, $\Delta\overline{x}_2 = \frac{1}{n-k}\sum_{k+1}^{n}\Delta x_i$.

Through the SIC method, the degradation information can be used to estimate the time when the change point of LEDs occurs. One of the disadvantages is that SIC tends to select fewer change points, which may cause important change points to be ignored and fail to fully capture the complex changes in the data. In addition, in the case of multiple change points, parameter estimation may be inaccurate, affecting the effectiveness of change point detection. Another disadvantage is that the change point can only be the test time, and the specific change point time is unknown. When using the Schwarz information criterion (SIC) for change point detection, we verified and confirmed the location of the change point by combining numerical results with graphical analysis. First, we plotted the LED degradation data into a time series graph. This allowed us to visually see the changing trend of the data, especially whether there were sudden changes or fluctuations in the degradation rate. Then, by calculating the SIC value at different change point positions, we plotted the changes in the SIC value over time. Usually, the SIC value would fluctuate significantly at the change point position, with a local minimum or inflection point appearing. The data segments corresponding to these inflection points changed greatly, indicating the potential change point location. Finally, the SIC method was combined with the intuitive observation value method to find the change point of LED LOP BE degradation.

3.4. Estimation of Parameter Values Under Accelerated Stress

For samples from the same batch, due to the differences in materials, production processes, etc., the individual drift coefficient can be considered to be μ, which is the degradation rate of LEDs, and the diffusion coefficient σ, which represents the random factors in the degradation of LEDs. Assume that the LED is exposed to a continuous stress accelerated degradation test, S_0 is the normal working stress level, S_k is the kth accelerated stress level, and the k value in this paper is 1–5. X_{ijk} is the jth measurement value of the ith sample under the kth accelerated stress. t_{ijk} is the time point at which the ith sample is measured for the jth time under the kth accelerated stress, where the value of i is 1–60, and the value of j is the number of measurements at different stresses in Table 3. The number of measurements under stresses S1–S5 is different. $\Delta X_{ijk} = X_{ijk} - X_{i(j-1)k}$ is the performance degradation amount, and $\Delta t_{ijk} = t_{ijk} - t_{i(j-1)k}$ is the time increment. Based on the properties of the Wiener process, we know that $\Delta X_{ijk} \sim N\left(\mu\Delta t_{ijk}, \sigma^2\Delta t_{ijk}\right)$. Since the above assumption is that the product performance degradation meets the multi-stage property, there are n_q measurement data of the n measurement data of each sample belonging to the performance degradation of the qth stage. Then, the maximum likelihood function is established for the measurement data $\left(\Delta X_{ijk}, \Delta t_{ijk}\right)$ of each stage, as follows in Equation (17):

$$L(\mu_{ik}, \sigma_{ik}) = \prod_{j=1}^{n_q}\frac{1}{\sqrt{2\pi\sigma_{ik}^2\Delta t_{ijk}}}\exp\left[-\frac{\left(\Delta X_{ijk} - \mu_{ik}\Delta t_{ijk}\right)^2}{2\sigma_{ik}^2\Delta t_{ijk}}\right] \quad (17)$$

According to above Equation (17), the maximum likelihood estimation can be used to estimate the square value of the drift coefficient and diffusion coefficient of each sample based on the multi-stage Wiener process: $\left(\mu_{ik}, \sigma_{ik}^2\right)$.

3.5. Construction of Multi-Stress Degradation Rate Model

High temperature causes the material to expand and stress to increase, while high humidity causes water vapor to invade the material. This situation will intensify the chemical decomposition or hydrolysis of the packaging material (such as epoxy resin, silicone), causing the packaging layer to lose its sealing properties, making metal wires and other materials more susceptible to oxidation and corrosion. When operating in a high temperature and high humidity environment, a high current will further increase the thermal burden of the chip and packaging materials, resulting in more heat accumulation, causing the internal temperature of the LED to continue to rise, leading to thermal aging and degradation of the material. The combined effect of high temperature and high current may cause the packaging material to crack under stress, affecting the sealing of the packaging and the overall performance of the LED. A high current will generate more heat, and in a high temperature environment, the heat dissipation effect of the LED will be affected, resulting in heat accumulation in the chip and packaging materials. This thermal accumulation effect will accelerate the degradation of the LED chip and increase the speed of brightness decay. In summary, it is necessary to consider the coupling effect of LED under different stresses.

The Arrhenius model is a significant framework in chemical kinetics and is extensively applied in accelerated testing models, as referenced in papers [19–22]. It typically describes the relationship between the degradation characteristic quantity and the individual temperature stress between products, which can be represented by Equation (18):

$$k(T) = \alpha_0 \exp(\frac{E_a}{k_B T}) \tag{18}$$

where k(T) represents the reaction rate, α_0, E_a, and k_B are constants representing the failure mechanism constant, the activation energy of the chemical reaction, and the Boltzmann constant, respectively, and T represents the reaction temperature in Kelvin.

Drawing on the Arrhenius model, Pham et al. studied the product reaction rate model under temperature and voltage, and temperature and humidity dual stress [23–25], as shown in Equation (19):

$$k(T, X_2) = \alpha_0 \exp(\frac{E_a}{k_B T}) \cdot \exp(\alpha_2 X_2 + \frac{\alpha_3' X_2}{k_B T}) \tag{19}$$

where X_2 represents voltage or humidity stress, $\alpha_3' X_2 / k_B T$ represents the coupling term of humidity stress or voltage stress, and α_2, α_3' are unknown parameters.

If the temperature stress is represented by X_1 and the stress coefficient term is represented by α_1, the product reaction rate model under double stress can be expressed as follows in Equation (20):

$$k(T, X_2) = \alpha_0 \exp(\alpha_1 X_1) \cdot \exp(\alpha_2 X_2) \cdot \exp(\alpha_3 X_1 X_2) \tag{20}$$

For better promotion, according to the above dual stress reaction rate model, the N stress reaction rate models based on the Arrhenius model will consist of individual stress terms such as temperature, humidity, current, etc., dual stress coupling terms such as temperature and humidity coupling terms, temperature, and current coupling terms, and so on. The three stress coupling terms until all stress coupling terms are the product of N terms, and the expression is as follows in Equation (21):

$$k(\alpha_1, \alpha_2, \ldots \alpha_N) = \alpha_0 \prod_{m=1}^{N} \exp(\alpha_m X_m) \times \prod_{\substack{m=1, n=1, m \neq n, m < n, \\ a = N+1, N+2, \ldots N+C_N^2}}^{N} \exp(\alpha_a X_m X_n) \times \prod_{\substack{m=1, n=1, p=1, m \neq n \neq p, m < n < p, \\ b = N+C_N^2+1, N+C_N^2+2, \ldots, N+C_N^3}}^{N} \exp(\alpha_b X_m X_n X_p) \times \cdots \exp(\alpha_N X_1 X_2 \cdots X_N) \quad (21)$$

where X_* represents N different forms of stress, α_* is an unknown parameter of the model, m < n is intended to ensure that the product terms do not include identical items. The first product term on the right side of the equation represents the effect of N distinct stresses on the reaction rate without coupling. In contrast, the second product term through to the last term on the right side indicates the potential impact of stress coupling on the reaction rate. According to [16], this type of LED has coupling effects in temperature, humidity, and current. For comparison, this paper calculates the two models of full stress coupling and uncoupled stress as follows in Equation (22):

$$\begin{aligned} &k_1(\alpha_{10}, \alpha_{11}, \alpha_{12}, \alpha_{13}) = \alpha_{10} \times \exp(\alpha_{11} X_1) \times \exp(\alpha_{12} X_2) \times \exp(\alpha_{13} X_3) \\ &k_2(\alpha_{20}, \alpha_{21}, \ldots, \alpha_{27}) = \alpha_{20} \times \exp(\alpha_{21} X_1) \times \exp(\alpha_{22} X_2) \times \exp(\alpha_{23} X_3) \times \\ &\exp(\alpha_{24} X_1 X_2) \times \exp(\alpha_{25} X_1 X_3) \times \exp(\alpha_{26} X_2 X_3) \times \exp(\alpha_{27} X_1 X_2 X_3) \end{aligned} \quad (22)$$

In the above Equation (22), k1 represents the degradation of LED LOP BE without considering coupling, k2 represents the degradation of LED LOP BE with considering full coupling, and α_{xy} represents the coefficient to be estimated. Among them, x represents the above two cases, and y represents the identifier of the value to be estimated.

In this paper, we believe that the value of the σ diffusion parameter is also related to the stress magnitude and has a strong coupling effect with temperature, humidity, and current stress. Therefore, according to Equation (22), we also estimate the unknown parameters in the diffusion parameter as follows in Equation (23):

$$\begin{aligned} &\sigma_1(\alpha_{30}, \alpha_{31}, \alpha_{32}, \alpha_{33}) = \alpha_{30} \times \exp(\alpha_{31} X_1) \times \exp(\alpha_{32} X_2) \times \exp(\alpha_{33} X_3) \\ &\sigma_2(\alpha_{40}, \alpha_{41}, \ldots, \alpha_{47}) = \alpha_{40} \times \exp(\alpha_{41} X_1) \times \exp(\alpha_{42} X_2) \times \exp(\alpha_{43} X_3) \times \\ &\exp(\alpha_{44} X_1 X_2) \times \exp(\alpha_{45} X_1 X_3) \times \exp(\alpha_{46} X_2 X_3) \times \exp(\alpha_{47} X_1 X_2 X_3) \end{aligned} \quad (23)$$

We then normalize the stress according to Equation (24) below.

$$\xi_i = \xi(S_i) = \frac{S_i - S_{i0}}{S_{iH} - S_{i0}} 1 \leq i \leq N \quad (24)$$

According to the above Equation (24), standardize the three stresses of temperature, humidity, and current are standardized as follows in Equation (25):

$$\begin{aligned} \xi_1 &= \xi\left(\frac{1}{T_i}\right) = \frac{\log\left(\frac{1}{T_i}\right) - \log\left(\frac{1}{T_{i0}}\right)}{\log\left(\frac{1}{T_{iH}}\right) - \log\left(\frac{1}{T_{i0}}\right)} \\ \xi_2 &= \xi(RH_i) = \frac{\log RH_i - \log RH_{i0}}{\log RH_{iH} - \log RH_{i0}} \\ \xi_3 &= \xi(I_i) = \frac{\log I_i - \log I_{i0}}{\log I_{iH} - \log I_{i0}} \end{aligned} \quad (25)$$

ξ_1 represents the standardization of temperature stress, and ξ_2 and ξ_3 indicate the normalization of humidity and current stress. It should be noted that the unit of temperature stress is Kelvin temperature.

3.6. Unified Paradigm of Multiple-Stress Acceleration Factor Model

The acceleration factor (AF) is used to quantify the rate at which a physical phenomenon is accelerated under different conditions. It is usually used in reliability analysis, life prediction, and accelerated testing [26,27]. The main application scenario of the acceleration factor of LEDs is in accelerated aging tests, where the failure time is shortened by increasing the temperature, humidity, current, or other stresses, using the shortest possible time to estimate its service life under rated working conditions. Assuming that the accelerated stress to which the LEDs are subjected is S, the ith and jth accelerated stress levels are S_i and S_j, and the product life under the accelerated stresses S_i and S_j are t_i and t_j respectively, and the acceleration factor of stress S_j equivalent to stress S_i can be defined as the following Equation (26):

$$AF_{ij} = \frac{t_j}{t_i} \tag{26}$$

Life is proportional to the reverse reaction rate in the model, according to Equation (21), and the relationship between life and stress can be obtained as Equation (27):

$$\begin{aligned} L(\alpha_1, \alpha_2, \ldots \alpha_N) = \alpha_0 \prod_{m=1}^{N} \exp(-\alpha_m X_m) \times & \prod_{\substack{m=1, n=1, m \neq n, m < n, \\ a = N+1, N+2, \ldots N + C_N^2}}^{N} \exp(-\alpha_a X_m X_n) \times \\ & \prod_{\substack{m=1, n=1, p=1, m \neq n \neq p, m < n < p, \\ b = N + C_N^2 + 1, N + C_N^2 + 2, \ldots, N + C_N^3}}^{N} \exp(-\alpha_b X_m X_n X_p) \times \cdots \exp(-\alpha_N X_1 X_2 \cdots X_N) \end{aligned} \tag{27}$$

After standardizing Equation (27), the following Equation (28) is obtained:

$$\begin{aligned} L(\alpha_1, \alpha_2, \ldots \alpha_N) = \alpha_0 \prod_{m=1}^{N} \exp(-\alpha_m \xi_m) \times & \prod_{\substack{m=1, n=1, m \neq n, m < n, \\ a = N+1, N+2, \ldots N + C_N^2}}^{N} \exp(-\alpha_a \xi_m \xi_n) \times \\ & \prod_{\substack{m=1, n=1, p=1, m \neq n \neq p, m < n < p, \\ b = N + C_N^2 + 1, N + C_N^2 + 2, \ldots, N + C_N^3}}^{N} \exp(-\alpha_b \xi_m \xi_n \xi_p) \times \cdots \exp(-\alpha_N \xi_1 \xi_2 \cdots \xi_N) \end{aligned} \tag{28}$$

According to Equation (25), the standardized unified paradigm of the multi-stress acceleration factor model can be expressed as the following Equation (29):

$$\begin{aligned} & AF(\alpha_0, \alpha_1, \ldots, \alpha_u) = \\ & \alpha_0 \prod_{m=1}^{N} \exp[\alpha_m(\xi_m - \zeta_{mu})] \times \prod_{\substack{m=1, n=1, m \neq n, m < n \\ b = N+1, N+2, \ldots, N + C_N^2}}^{N} \exp[\alpha_b(\xi_m \xi_n - \xi_{mu} \xi_{nu})] \\ & \times \prod_{\substack{m=1, n=1, p=1, m \neq n \neq p, m < n < p \\ b = N + C_N^2 + 1, N + C_N^2 + 2, \ldots, N + C_N^3}}^{N} \exp\left[\alpha_c\left(\xi_m \xi_n \xi_p - \xi_{mu} \xi_{nu} \xi_{pu}\right)\right] \\ & \times \cdots\cdots \times \exp[\alpha_u(\xi_1 \xi_2 \cdots \xi_N - \xi_{1u} \xi_{2u} \cdots \xi_{Nu})] \end{aligned} \tag{29}$$

where ξ_{*u} represents the stress level of a normal working state. In particular, the acceleration factor model under three stresses can be expressed as the following Equation (30):

$$\begin{array}{l} AF(\alpha_0, \alpha_1, \ldots, \alpha_7) \\ = \frac{k(\alpha_0,\alpha_1,\ldots,\alpha_7)}{k_u(\alpha_0,\alpha_1,\ldots,\alpha_7)} = \exp[\alpha_1(\xi_1 - \xi_{1u})] \cdot \exp[\alpha_2(\xi_2 - \xi_{2u})] \\ \cdot \exp[\alpha_3(\xi_3 - \xi_{3u})] \cdot \exp[\alpha_4(\xi_1\xi_2 - \xi_{1u}\xi_{2u})] \cdot \exp[\alpha_5(\xi_1\xi_3 - \xi_{1u}\xi_{3u})] \\ \cdot \exp[\alpha_6(\xi_2\xi_3 - \xi_{2u}\xi_{3u})] \cdot \exp[\alpha_7(\xi_1\xi_2\xi_3 - \xi_{1u}\xi_{2u}\xi_{3u})] \end{array} \quad (30)$$

4. Reliability Evaluation of LED LOP BE Degradation Performance

Based on the performance degradation data of 300 samples from S1 to S5 under various stresses, we can determine whether the LED LOP BE meets the Wiener process. Since the data measurement of the samples in the experiment is not measured at equal intervals, that is, Δt_j under each group of stress levels is not a fixed value. According to the characteristic $\Delta X_j \sim N(\mu_{ik}\Delta t_j, \sigma_{ik}^2\Delta t_j)$ of the Wiener process, a goodness of fit test on ΔX_j can be performed to determine whether the degradation increment of each sample at each stage obeys the normal distribution, thereby determining whether its degradation process obeys the Wiener process. The Shapiro–Wilk test is a statistical method used to detect whether sample data come from a normal distribution. It is mainly used to test the normality of data, but it cannot directly detect whether the data come from other specific distributions. It is particularly effective for small sample data (3–5000 sample size). This paper used the Shapiro–Wilk statistic to perform a hypothesis test with a confidence level of 95%. A total of 107 groups of degradation quantities under five accelerated stresses all obeyed the normal distribution, so the normal distribution model was selected to model each group of degradation quantities.

Since the measured LED LOP BE degradation was staged, the next step was to determine the location of the change point. Based on SIC, the change points of the three stages under S1–S5 stress were found, but some of the change points were inaccurate. Based on SIC detection and visual observation, this paper finally determined the S1–S5 stress change points as shown in Table 4.

Table 4. SIC change point under S1–S5 stress, visual change point, and final choice.

Test Stress Level	SIC Change Point	Visual Change Point	Final Choice
S1 (85 °C 45%RH 20 mA)	1033 h 3105 h	2091 h 4416 h	2091 h 4416 h
S2 (85 °C 85%RH 20 mA)	1487 h 4416 h	1487 h 4416 h	1487 h 4416 h
S3 (85 °C 85%RH 220 mA)	1033 h 1846 h	1033 h 1846 h	1033 h 1846 h
S4 (95 °C 45%RH 525 mA)	264 h 696 h	264 h 744 h	264 h 696 h
S5 (150 °C 45%RH 300 mA)	456 h 792 h	72 h 648 h	72 h 648 h

The SIC change points under S1 and S5 stresses were problematic, because, according to the test data, the greater the stress, the shorter the first stage of degradation time and the less obvious it was. Therefore, the first change point time of S1 should be greater than 1487 h. According to Figure 3a, we chose 2091 h as the first change point. The second change point may not be 4416 h because the time interval of the test was large after more than 1000 h. However, the test did change after 4416 h, so this paper set the second change points of S1 and S2 to 4416 h. The actual situation may be that the second stage change points under S1 and S2 stresses were less than 4416 h, and the second change point time under S2 stress was earlier than the second change point time under S1 stress. The first stage under S5 stress should also be less than 264 h. According to the degradation image, we chose 72 h as the first change point under S5 stress. The second change point time under S4 stress was not obvious to the naked eye, so the S4 change point still chose the original change point of SIC detection. The second change point under S5 stress should be earlier than the second change point under S4 stress. Based on Figures 3 and 4, we determined 648 h as the second change point of S5 stress.

Substituting the measured data $\left(\Delta X_{ijk}, \Delta t_{ijk}\right)$ into Equation (17), the parameter values of each sample in stage 1, stage 2, and stage 3 were obtained as shown in Tables 5–7.

From Table 5, we found that, in the first stage, high stress led to a larger diffusion coefficient. From Table 6, we can see that the diffusion coefficient under stress S5 in the second stage was significantly greater than the diffusion coefficients of S1–S4, but the diffusion coefficients of S1–S4 did not have an obvious pattern. There was also no obvious pattern in the diffusion coefficients under stresses S1–S5 in the third stage. We checked the data from the final stages using the Shapiro–Wilk information criterion and found that the data conformed to the normal distribution, which meant that the hypothesis was correct.

After estimating the drift coefficient and the square value of the diffusion coefficient of each sample based on the multi-stage Wiener process, the estimated values of the unknowns without considering stress coupling and considering full stress coupling are as shown in Tables 8 and 9, according to Equation (22).

Table 5. (μ, σ^2) of each sample in the first stage under accelerated stress.

	S1		**S2**		**S3**		**S4**		**S5**	
	μ	σ^2	μ	σ^2	μ	σ^2	μ	σ^2	μ	σ^2
1	−0.00064	0.0000022	0.00020	0.000019	−0.00053	0.000015	−0.00080	0.000028	−0.01722	0.00086
2	−0.00059	0.0000051	0.00035	0.000018	−0.00039	0.000012	−0.00131	0.000017	−0.01989	0.00090
3	−0.00066	0.0000048	−0.00087	0.000008	−0.00106	0.000040	−0.00073	0.000029	−0.02004	0.00097
4	−0.00079	0.0000053	−0.00089	0.000016	−0.00042	0.000015	−0.00104	0.000020	−0.01335	0.00057
...	...	...	...	...	...	...	...	...	...	...
60	−0.00066	0.0000022	−0.00102	0.000014	−0.00040	0.000016	−0.00170	0.000018	−0.01769	0.00084

Table 6. (μ, σ^2) of each sample in the second stage under accelerated stress.

	S1		**S2**		**S3**		**S4**		**S5**	
	μ	σ^2	μ	σ^2	μ	σ^2	μ	σ^2	μ	σ^2
1	−0.00245	0.000081	−0.00299	0.000019	−0.00433	0.000000002	−0.00564	0.000009	−0.00805	0.00002
2	−0.00249	0.000063	−0.00304	0.000024	−0.00493	0.000003	−0.00656	0.000008	−0.00838	0.00002
3	−0.00236	0.000079	−0.00311	0.000010	−0.00406	0.0000004	−0.00705	0.000010	−0.00824	0.00002
4	−0.00241	0.000103	−0.00374	0.000002	−0.00374	0.0000002	−0.00725	0.000009	−0.00836	0.00002
...	...	...	...	...	...	...	...	...	...	...
60	−0.00207	0.000006	−0.00355	0.00000004	−0.00453	0.00000002	−0.00707	0.000013	−0.00832	0.00002

Table 7. (μ, σ^2) of each sample in the third stage under accelerated stress.

	S1		**S2**		**S3**		**S4**		**S5**	
	μ	σ^2	μ	σ^2	μ	σ^2	μ	σ^2	μ	σ^2
1	−0.00047	0.000019	−0.00012	0.000000005	−0.00199	0.000003	−0.01119	0.000016	−0.00577	0.0000001
2	−0.00035	0.000019	−0.00020	0.000000002	−0.00220	0.00002	−0.01222	0.000006	−0.00401	0.000003
3	−0.00034	0.000018	−0.00029	0.0000007	−0.00127	0.00000007	−0.01166	0.000007	−0.00379	0.000001
4	−0.00037	0.000013	−0.00025	0.00000004	−0.00124	0.000006	−0.00913	0.000056	−0.00362	0.000005
...	...	...	...	...	...	...	...	...	...	...
60	−0.00036	0.000011	−0.00024	0.0000062	−0.00069	0.0000076	−0.01078	0.000015	−0.00331	0.000006

Table 8. Estimated values of unknowns in (μ, σ^2) without considering stress coupling.

Unknown Parameters	Stage 1 μ	Stage 2 μ	Stage 3 μ
α_{10}	0.007014750	−0.003712422	−0.000019466
α_{11}	−0.000972560	−0.164774484	0.778742624
α_{12}	−2.431556556	−0.635719572	−2.767013425
α_{13}	−0.001422939	1.283464151	6.602109318
Total error	0.000282137	0.000007291	0.000008037
α_{30}	0.000127708	0.000129637	0.000032910
α_{31}	−0.668988832	−0.669001168	−0.669000382
α_{32}	−0.633587575	−0.633580772	−0.633581699
α_{33}	−0.597809237	−0.597823584	−0.597817233
Total error	0.000000120	0.000000005	0.000000001

Table 9. Estimated values of unknowns in (μ, σ^2) without considering full stress coupling.

Unknown Parameters	Stage 1 μ	Stage 2 μ	Stage 3 μ
α_{20}	−0.000667902	−0.008121391	−0.007065198
α_{21}	−0.627356055	−0.030382051	−0.089405067
α_{22}	−0.615998179	−0.520015567	−0.924158836
α_{23}	−0.584547350	−0.008157158	−0.013968919
α_{24}	−0.587455832	−0.073466467	−0.666206818
α_{25}	−0.571143264	−0.010147002	−0.020034556
α_{26}	−0.564365828	−0.015923113	−0.041549123
α_{27}	−0.557248131	−0.021189437	−0.057958340
Total error	0.000310345	0.000034388	0.000044228
α_{40}	0.000154468	0.000523843	0.000076408
α_{41}	−1.292420481	−1.292396421	−1.292455161
α_{42}	−1.219442627	−1.219416120	−1.219463372
α_{43}	−1.095819224	−1.095844943	−1.095857939
α_{44}	−1.124825010	−1.124819070	−1.124846588
α_{45}	−1.055187472	−1.055222283	−1.055231056
α_{46}	−1.040846948	−1.040856322	−1.040865845
α_{47}	−1.023492453	−1.023505562	−1.023511556
Total error	0.000000128	0.000000006	0.000000002

According to Tables 8 and 9, the LOP BE degradation rate and random variation under normal stress levels (25 °C, 40%RH, 10 mA) were extrapolated. According to Equations (22), (23), and (25), the average degradation value under normal stress level was actually α_{10} and α_{20}. It should be noted that this value was the degradation value of 24 h, not the degradation value per hour.

According to Formula (30), we calculated that the AF of the first stage under S1 stress was 0.389, and the AF of the second stage was 0.795. According to Equation (26), the time of the first stage under normal stress was 5375.321 h, and the time of the second stage was 2924.528 h. Then, according to the failure value of LOP BE reaching 0.695, without considering stress coupling, the time of the third stage was about 11,700 h. Figure 5 below shows the degradation diagram of LED LOP BE over time without considering stress coupling and random changes considering full stress coupling but not considering random changes, and the historical failure scatter points.

As can be seen from Figure 5, the LED life was about 20,000 h without considering stress coupling, and 5848 h with stress coupling, which was more consistent with the historical life scatter points of 5305 h to 6992 h. According to the Monte Carlo simulation, the life was 5592.35–5975.52 h with coupling and random factors. It may be that the LEDs

entered the third stage, resulting in an extended degradation time. However, if stress coupling was not considered, the LED's life would be seriously overestimated.

This paper did not draw the LOP BE curve of LEDs without considering the degradation stage, because the situation without considering the degradation stage was inaccurate. This paper also made an LOP BE degradation rate of 60 samples under normal stress levels (25 °C, 40%RH, 10 mA). The improvement of LOP BE of LEDs around 1000 h was 9–16%, which was close to the calculated 15% without considering coupling. Through the blue broken line in Figure 5, without considering stress coupling, the average life of LEDs was 20,330 h, which meets the 20,000 h standard adopted by manufacturers for LEDs. However, the life of LEDs in reality is worrying, and the historical life scatter points did not exceed 7000 h at most, considering that stress coupling is also closer to the real life of LEDs. However, the degradation of life is also problematic. After all, the real life of LEDs includes many aspects, not only degradation failure but also occasional failure. Degradation failure may include more stress combinations, such as salt spray at the seaside, alternating hot and cold climates, etc. Occasional failure includes external vibration, the number of power switches, etc. There are also some problems in the experimental design of this paper. The failure mechanism does not change under S1–S5 stress degradation, but whether the three stresses of constant temperature, humidity, and current represent the degradation of real-world LEDs and the impact of high temperature on high humidity are the issues to be studied in the next step. However, certainly, the gap between the actual situation and not considering the coupling of stress is still too large. It can be seen that the consideration of coupling has a strong influence on the evaluation of the degradation and life of LEDs; therefore, it is necessary to consider the coupling effect between multiple stresses in the life assessment.

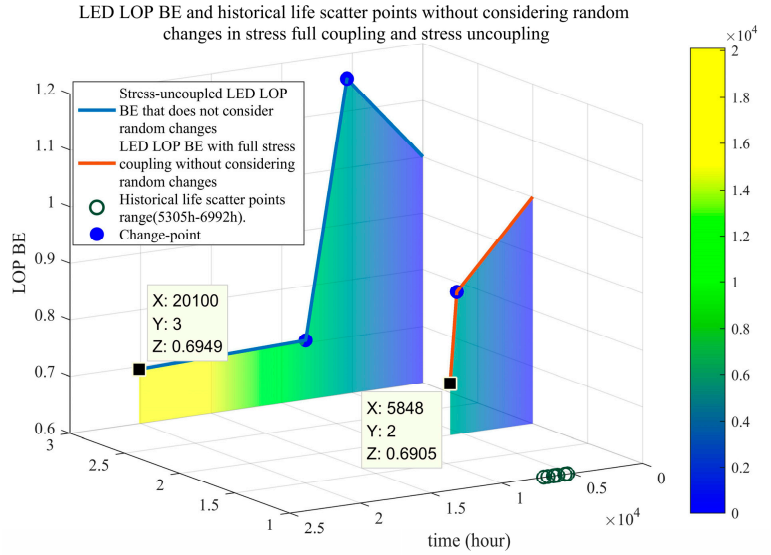

Figure 5. Degradation curve and historical scatter points without considering random factors.

5. Conclusions

According to the multi-stage characteristics of the LED degradation process, this paper proposes a multi-stage Wiener process degradation model under generalized coupling accelerated stress. First, LOP is selected as the degradation characteristic quantity according to the accelerated degradation test, and it is determined to be in line with the normal distribution. Then, the multi-stage Wiener process degradation parameters are estimated, and a generalized coupling model is established. Finally, the degradation life of LEDs under normal temperature stress is extrapolated according to the multi-stress acceleration factor. According to the historical scatter points, it is verified that the LED's degradation cannot ignore the coupling of three stresses.

This article only considers the effects of temperature, humidity, and current on LED LOP BE degradation, but the actual degradation also has multiple stress components, such as low temperature, alternating hot and cold, switching times, static electricity, etc. It also includes the effects of differences in process or material quality of different LED manufacturers, the effects of continuous drying at high temperatures and self-heating of LEDs at high temperatures on humidity, etc., and the competitive failure of unexpected failures that may occur during the degradation process and the degradation failure of LEDs' structure under multi-stress coupling and degradation of LEDs at different degradation stages under different stress coupling are also good research directions. LED testing methods that use alternating hot and cold and cyclic loads are more in line with the actual environment than constant stress accelerated degradation tests.

Author Contributions: Conceptualization, Y.D. and Z.Z.; methodology, Y.D., Z.Z. and H.D.; software, Y.D.; validation, Y.D. and H.D.; investigation, Z.Z. and H.D.; writing—original draft preparation, Y.D. and K.L.; writing—review and editing, Y.D. and Z.Z. All authors have read and agreed to the published version of the manuscript.

Funding: This research received no external funding.

Data Availability Statement: Data are contained within the article.

Acknowledgments: Thanks to all of the authors cited in this article and the referees for their helpful comments and suggestions.

Conflicts of Interest: The authors declare no conflicts of interest.

References

1. Liao, L.; Kottig, F. Review of hybrid prognostics approaches for remaining useful life prediction of engineered systems, and an application to battery life prediction. *IEEE Trans. Reliab.* **2014**, *63*, 191–207. [CrossRef]
2. Jing, B.; Cui, Z. Online life prediction of the fuel pump based on failure physics and data-driven fusion. *Chin. J. Sci. Instrum.* **2022**, *43*, 68–76.
3. Tao, T.; Zio, E.; Zhao, W. A novel support vector regression method for online reliability rediction under multi-state varying operating conditions. *Reliab. Eng. Syst. Saf.* **2018**, *77*, 35–49. [CrossRef]
4. Kaaya, I.; Koehl, M.; Mehilli, A.P. Modeling outdoor service lifetime prediction of PV modules: Effects on PV module power of combined climatic stressors degradation. *IEEE J. Photovolt.* **2019**, *9*, 1105–1112. [CrossRef]
5. Mehr, M.Y.; Van Driel, W.D.; Zhang, G.Q. Reliability and lifetime prediction of remote phosphor plates in solid-state lighting applications using accelerated degradation testing. *Electron. Mater.* **2016**, *45*, 444–452. [CrossRef]
6. Fu, K.; Chu, T. Lifetime predictions of LED-based light bars by accelerated degradation test. *Microelectron. Reliab.* **2012**, *52*, 1332–1336.
7. Miao, H.; Guo, W. Lifetime prediction of UV LEDs based on Bayesian MCMC and other models. *Acta Opt. Sin.* **2024**, *44*, 2223001.
8. Liang, B.; Wang, Z.; Qian, C. Investigation of step-stress accelerated degradation test strategy for ultraviolet light emitting diodes. *Materials* **2019**, *12*, 3119. [CrossRef]
9. Wang, P.; Tang, Y.; BAE, S.J. Bayesian analysis of two-phase degradation data based on change-point Wiener process. *Reliab. Eng. Syst. Saf.* **2017**, *170*, 244–256. [CrossRef]
10. Pan, Z.; Balakrishnan, N.; Sun, Q. Bivariate degradation analysis of products based on Wiener processes and copulas. *J. Stat. Comput. Simul.* **2013**, *83*, 1316. [CrossRef]
11. Wang, W. A model for residual life prediction based on Brownian motion with an adaptive drift. *Microelectron. Reliab.* **2011**, *51*, 285. [CrossRef]
12. Si, X.; Wang, W.; Hu, C. Remaining useful life estimation based on a nonlinear diffusion degradation process. *IEEE Trans. Reliab.* **2012**, *61*, 50. [CrossRef]
13. Li, G.; Zhang, J. Life prediction method of motor ground-wall insulation material based on Wiener process. *Electr. Mach. Control* **2023**, *27*, 40–47.
14. Meneghini, M.; Podda, S.; Morelli, A.; Pintus, R.; Trevisanello, L.; Meneghesso, G. High brightness GaN LEDs degradation during DC and pulsed stress. *Microelectron. Reliab.* **2006**, *46*, 1720–1724. [CrossRef]
15. *IES TM-28-14*; Projecting Long-Term Luminous Flux Maintenance of LED Lamps and Luminaires. IES-USA: New York, NY, USA, 2014.
16. Dong, Y.; Zhou, Z. Multi-Stress Accelerated Degradation Testing Reliability Assessment of LED Lamp Beads Considering Generalized Coupling. *Appl. Sci.* **2024**, *14*, 8767. [CrossRef]
17. Liu, Y.; Wang, Y. A new universal multi-stress acceleration model and multi-parameter estimation method based on particle swarm optimization. *Proc. Inst. Mech. Eng. Part O J. Risk Reliab.* **2020**, *234*, 764–778. [CrossRef]

18. Khan, A.; Hwang, S.; Lowder, J. Reliability issues in AlGaN based deep ultraviolet light emitting diodes. In Proceedings of the IEEE 47th Annual International Reliability Physics Symposium, San Jose, CA, USA, 26 April 2009; pp. 89–93.
19. Wang, M.; Wang, S. Reliability analysis of ball screw based on double-stress accelerated life testing. *J. Beijing Univ. Chem. Technol.* **2022**, *48*, 703–709.
20. Kang, Q.; Li, Y. Reliability estimation of thin film platinum resistance MEMS thermal mass flowmeter by step-stress accelerated life testing. *Microelectron. Reliab.* **2023**, *147*, 115026. [CrossRef]
21. Amleh, M.A.; Raqab, M.Z. Inference in simple step-stress accelerated life tests for Type-II censoring Lomax data. *J. Stat. Theory Appl.* **2021**, *20*, 364–379. [CrossRef]
22. Abd El-Raheem, M.A.M.; Abu-Moussa, M.H. Accelerated Life Tests under Pareto-IV Lifetime Distribution: Real Data Application and Simulation Study. *Mathematics* **2020**, *8*, 1786. [CrossRef]
23. Pascual, F.; Meeker, W.; Escobar, L. Accelerated life test models and data analysis. In *Springer Handbook of Engineering Statistics*; Pham, H., Ed.; Springer: London, UK, 2006; pp. 397–426.
24. Indmeskine, F.E.; Saintis, L.; Kobi, A. Review on accelerated life testing plan to develop predictive reliability models for electronic components based on design-of-experiments. *Qual. Reliab.* **2023**, *39*, 2594–2607. [CrossRef]
25. Nassar, M.; Dobbah, S.A. Inference on Constant Stress Accelerated Life Tests Under Exponentiated Exponential Distribution. *Electron. J. Appl. Stat. Anal.* **2023**, *16*, 234–256.
26. Wang, H.; Zhou, Y.; Teng, F. Optimization Design of Accelerated Degradation Testing Based on the Principle of Constant Acceleration Factors. *J. Mech. Eng.* **2018**, *54*, 212–219. [CrossRef]
27. Gai, B.; Teng, K.; Wang, H. Reliability assessment approach for Wiener-type degradation based on acceleration factor. *Tactical Missile Technol.* **2017**, *25*, 25–30.